Table I. Maximum Vibrational Circular Dichroism Intensity for L-Amino Acids[a]

amino acid	$10^4\Delta\epsilon$, cm^{-1} L mol^{-1}	frequency, cm^{-1}
alanine	11.3 ± 0.2	2968
serine	3.3	2963
cysteine	8.8	2972
histidine	5.1	2979
phenylalanine	5.0	2975
valine	7.3	2972
penicillamine	8.9	2963
methionine	6.5	2975
proline	7.3	2995
hydroxypyroline	9.1	2989
allo-hydroxyproline	7.6	2968
threonine	11.0	2978
allo-threonine	4.9	2968
leucine	16.0	2963
isoleucine	15.3	2972
aspargine	5.9	2972
glutamine	5.3	2976
lysine hydrochloride	5.1	2976
arginine hydrochloride	4.7	2966

[a] The absorption strength for the C^*_α–H modes is estimated to be $\epsilon \cong 3$–5 on the basis of spectra for alanine-*C*-d_3, serine, cysteine, and aspargine.

hydrogen bonding would be disrupted.

The methine C^*_α–H stretching chirality rule can also be extended to α-L-hydroxy acids, such as L-lactic acid[9] and (*S*,*S*)-tartaric acid,[10] and to bis(L-amino acid)copper(II) complexes[5f,g] where currents are induced by C^*_α–H motion in the ring fragments $\overline{C^*_\alpha CO \cdots DO}$ (**2**) and $\overline{C^*_\alpha CO\text{–}Cu\text{–}N}$, respectively. The ring fragment in the hydroxy acids is isoelectronic and nearly equivalent in mass distribution to the amino acid ring. The VCD bias in the hydroxy acids is approximately the same as in the amino acids whereas the Cu complexes show a bias that is approximately twice as large.[5f,g]

The anisotropy ratio $\Delta\epsilon/\epsilon$ for the methine C^*_α–H stretching mode in the molecules discussed here and in Table I is either measured or estimated to be greater than $+1 \times 10^{-4}$. Molecules that cannot form intramolecular hydrogen bonds for which C^*_αH stretching VCD is available show intensity with $\Delta\epsilon/\epsilon$ less than 10^{-4}. Examples are 2,2,2-trifluoro-1-phenylethanol (neat and in CCl_4 solution),[11] neopentyl-*1*-*d* chloride,[11a] deuterated phenylethanes,[12] and other phenylethane derivatives.[13] The CH stretching VCD of (*S*,*S*)-dimethyl tartrate[1d] is predominantly C^*_α–H stretch and has a $\Delta\epsilon/\epsilon$ for this mode of $\sim+1.5 \times 10^{-4}$, equal in sign and magnitude to (*S*,*S*)-tartaric acid and L-lactic acid.[14] This strongly implies a conformation comprised of two isolated hydrogen-bonded rings rather than the interlocking hydrogen-bonded ring conformation,[2b-d] since, in the latter, two opposing ring currents would cancel.

The methine chirality rule appears to be a promising interpretive concept for VCD spectra and it reveals that VCD intensities can be particularly sensitive to the presence and strength of intramolecular hydrogen bonds. The rule may likely be further generalized to include any out-of-plane stretching motion associated with an adjacent induced ring current.

Acknowledgment. This research was supported by grants from the National Institutes of Health (GM-23567) and the National Science Foundation (CHE 83-02416).

Registry No. L-Alanine, 56-41-7; L-serine, 56-45-1; L-cysteine, 52-90-4; L-histidine, 71-00-1; L-phenylalanine, 63-91-2; L-valine, 72-18-4; L-penicillamine, 1113-41-3; L-methionine, 63-68-3; L-proline, 147-85-3; L-hydroxyproline, 51-35-4; L-*allo*-hydroxyproline, 618-27-9; L-threonine, 72-19-5; L-*allo*-threonine, 28954-12-3; L-leucine, 61-90-5; L-isoleucine, 73-32-5; L-aspargine, 70-47-3; L-glutamine, 56-85-9; L-lysine hydrochloride, 10098-89-2; L-arginine hydrochloride, 15595-35-4.

(9) Nafie, L. A. *Appl. Spectrosc.* **1982**, *36*, 489.
(10) Sugeta, H.; Marcott, C.; Faulkner, T. R.; Overend, J.; Moscowitz, A. *Chem. Phys. Lett.* **1976**, *40*, 397.
(11) (a) Holzwarth, G.; Hsu, E. C.; Mosher, H. S.; Faulkner, T. R.; Moscowitz, A. *J. Am. Chem. Soc.* **1974**, *96*, 252. (b) Nafie, L. A.; Cheng, J. C.; Stephens, P. J. *Ibid.* **1975**, *97*, 3842. (c) Nafie, L. A.; Keiderling, T. A.; Stephens, P. J. *Ibid.* **1976**, *98*, 2715.
(12) Havel, H. A. Ph.D. Thesis, University of Minnesota, Minneapolis, MN, 1981.
(13) Su, C. N.; Keiderling, T. A. *Chem. Phys. Lett.* **1981**, 77, 494.
(14) L-Lactic acid corresponds to "*S*" absolute configuration and is analogous in configuration to (*S*,*S*)-tartaric acid.

First Experimental Demonstration of Chemical Resonance in an Open System

F. Buchholtz and F. W. Schneider*

Institute of Physical Chemistry
University of Würzburg
D-8700 Würzburg, GFR
Received May 31, 1983

The phenomenon of resonance is observed when a damped oscillator is driven by a periodic driving force in such a way that the response amplitude of the oscillator goes through a maximum as a function of driving frequency.[1] The maximum occurs when the driving frequency is close to the endogeneous frequency of the oscillator if the damping constant is smaller than the endogeneous frequency. This is exemplified by many spectroscopic resonance processes familiar to every chemist. The mathematical equation for a damped oscillator is $f(t) = e^{-t/\tau} \cos(\omega_0 t)$ where $1/\tau$ is defined as the damping constant γ and ω_0 as the endogeneous frequency of the oscillator. We have asked ourselves whether resonance may also be demonstrated in a chemical reaction, i.e., when the driven system represents a chemical oscillator.[2] We report to our knowledge the first experimental example of chemical resonance as it occurs in the well-known Belousov–Zhabotinsky (BZ)[3] reaction, which is modified by the addition of Br^- and carried out in a continuous-flow stirred tank reactor (CSTR). In order to obtain chemical resonance, it was essential for us to conduct the BZ reaction in the absence of limit-cycle oscillations and to choose conditions that it only shows *damped* oscillations. We found such conditions guided by our computer simulations of chemical resonance in the Oregonator model (and other mechanisms).[2]

The BZ reaction is initiated inside the CSTR and run for a number of periods without inflow of reactants, i.e., $k_f = 0$, where k_f is the inverse mean residence time τ_r of all species in the absence of a chemical reaction, and $k_f = 1/\tau_r$ where $\tau_r = V/u$, V being the volume of the CSTR (1.70 mL) and u being the volume rate of flow expressed in mL/min. Two solutions are allowed to flow simultaneously from two motor-driven 50-mL syringes into the CSTR, which has been placed into a spectrometer in order to monitor the Ce^{4+} concentration at 350 nm as a function of time inside the reactor. One solution contains potassium bromide (2.4×10^{-6} M) and 0.6 M malonic acid in 0.75 M H_2SO_4 and the second solution contains 1×10^{-3} M Ce^{3+} and 0.28 M $KBrO_3$. The effective concentrations inside the reactor are half of the input concentrations, since two identical supply syringes and tubes are used. Any interference of the 350-nm light intensity with the kinetics of the present reaction could not be observed. The reaction mixture does not show any fluorescence.

We superimpose a sinusoidal modulation on the total flow through the CSTR. This is achieved by controlling flow frequency and amplitude via a CBM Commodore computer whose analog-converted output drives the step motor of a precise syringe pump (Infors Precidor). The time dependent flow rate is

$$k_f = k_f^0(1 + \alpha \cos \omega t)$$

where k_f^0 is the flow-rate constant in the absence of any modu-

(1) Minorsky, N. "Nonlinear Oscillations"; Van Nostrand: Princeton, NJ, 1962.
(2) Buchholtz, F., Diplomarbeit, University of Würzburg, 1981.
(3) Belousov, B. P. *Ref. Radiats. Med.* **1958**, *1959*, 145. Zhabotinsky, A. M. *Biofizika* **1964**, *9*, 306.

0002-7863/83/1505-7450$01.50/0

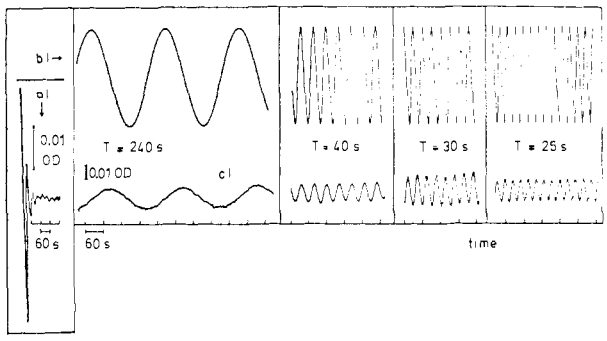

Figure 1. (a) Damped BZ oscillation: OD (350 nm) vs. time for $k_f^0 = 1.4 \times 10^{-3}$ s^{-1} and $\alpha = 0.5$. The period of the damped oscillation is $T \approx 35$ s ($\omega_0 \approx 0.18$ s^{-1}), and from the envelope, the damping constant is $\gamma \approx 0.04$ s^{-1} corresponding to $\tau \approx 25$ s. The resulting steady state is stable and nonoscillatory. (b) Time-dependent inflow $k_f(t)$ (forcing function) vs. time for constant flow (part a) and for the selected periods $T = 240$, 40, 30, and 25 s for $k_f^0 = 1.4 \times 10^{-3}$ s^{-1} and $\alpha = 0.5$. (c) Absorption of Ce^{4+} (OD at 350 nm) (response function) vs. time for identical conditions as in (b). The response amplitude (at the steady state) varies with frequency.

lation, α is the amplitude, and ω is the modulation frequency.

Figure 1a shows an example of a damped oscillation that has been obtained in the presence of Br^- at a constant inflow for $k_f^0 = 1.4 \times 10^{-3}$ s^{-1} corresponding to $\tau_r = 11.9$ min. Its damping constant is $\gamma \approx 0.04$ s^{-1} and the frequency is $\omega_0 \approx 0.18$ s^{-1} corresponding to a period of $\sim$35 s. The resulting (nonoscillatory) steady state is stable. This steady state is perturbed sinusoidally by a modulated flow rate whose period T varies between 10 and 240 s with $\alpha = 0.5$ at $k_f^0 = 1.4 \times 10^{-3}$ s^{-1} (trace b in Figure 1). The absorption of Ce^{4+} is recorded simultaneously at 350 nm (trace c in Figure 1). As expected both modulation and response periods are identical. The response amplitude is measured after attainment of the steady state. When the square of the response amplitude of Ce^{+4} is plotted point by point vs. the modulation frequency of the sinusoidal inflow, a chemical resonance curve is obtained. It represents a power or energy spectrum (Figure 2a). Its resonance maximum occurs at $\omega_0 = 0.21$ s^{-1} in close agreement with the frequency of the damped oscillator (Figure 1a). It is seen that the experimental resonance curve may be well fitted around the maximum by a Lorentz function. The bandwidth at half maximum is approximately twice the damping constant ($2\gamma = 0.08$ s^{-1}), which agrees well with the damping constant as determined in the time domain from the envelope of the damped oscillation (Figure 1a).

This procedure is equivalent to a "chemical" Fourier transformation from the time (Figure 1a) to the frequency (Figure 2a) domain. It is also possible to determine the experimental absorption and dispersion curves by making use of the experimental phase shift that exists between forcing function (Figure 1b) and forced solution (Figure 1c). The dispersion curve (Figure 2b) corresponds to the in-phase amplitude of the response curve whereas the absorption curve (Figure 2c) represents the 90° out-of-phase amplitude as a function of frequency.[4] Whereas the agreement between the experimental and the theoretical Lorentz absorption curves is good, there is a discrepancy of unknown origin in the fit to the dispersion curve at low frequencies. It is seen that the absorption curve is proportional to the power spectrum as expected.[4] We attribute the experimental rise of the curves at zero frequency to a slow superimposed exponential relaxation with which the BZ reaction relaxes to its steady state in addition to showing damped oscillations. The Fourier transform of an exponential relaxation corresponds to (the positive) half of a Lorentz function whose $\omega_0' = 0$, which was used to fit the experiment at low frequency (Figure 2).

In order to compare experiment with existing models we performed numerical integrations of the modified Oregonator

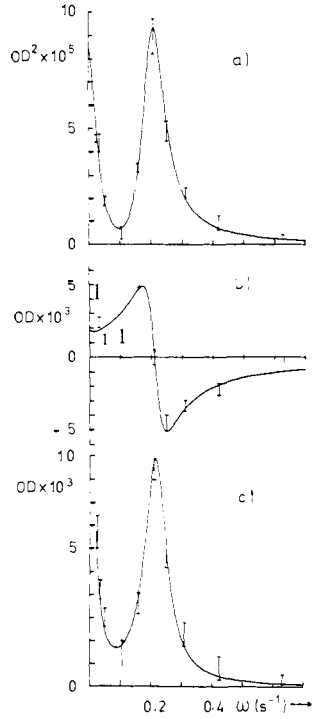

Figure 2. (a) Chemical resonance curve (power spectrum). Square of the response amplitude (Figure 1c) of Ce^{4+} (in OD units) vs. inflow frequency ω(s^{-1}) fitted by a Lorentz curve (solid curve); $\omega_0 \approx 0.21$ s^{-1}; half width at half maximum is $\gamma \approx 0.04$ s^{-1}; the experimental rise at $\omega \rightarrow 0$ has been fitted by the positive half of a Lorentz function whose $\omega_0' = 0$. (b) Dispersion spectrum obtained from the inphase amplitude of the response curve (Figure 1c) with respect to the forcing function (Figure 1b). Solid curve represents a calculated dispersion curve. (c) Absorption spectrum obtained from the 90° out-of-phase amplitude of the response curve (Figure 1c) with respect to the forcing function (Figure 1b); the solid curve represents a calculated Lorentz absorption curve.

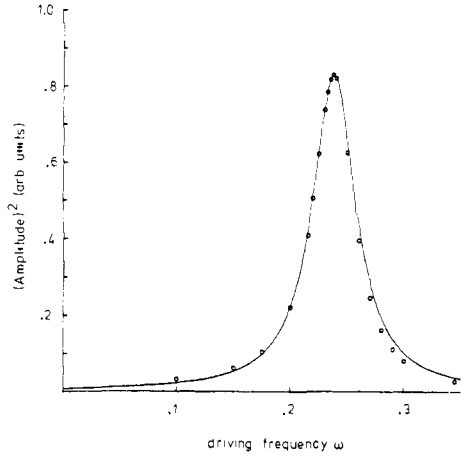

Figure 3. Chemical resonance curve (power spectrum) of the Oregonator model in the CSTR with rate constants and concentrations of Showalter et al.[5] (points); the solid curve represents a fitted Lorentz power spectrum.

mechanism[5] (not shown here), and Fourier transformed the numerical solutions. Chemical resonance was obtained as expected (Figure 3) for the special case when the Oregonator behaves like a damped oscillator in the CSTR and when Showalter et al.'s[5] rate constants and concentrations were used. However, when our different experimental set of concentrations was employed in the calculations, resonance was not obtained. Interestingly, the experimental rise at $\omega = 0$ was not predicted by the numerical

(4) Marshall, A. G. "Biophysical Chemistry"; Wiley: New York, 1978; p 370.

(5) Showalter, K.; Noyes, R. M.; Bar-Eli, K. *J. Chem. Phys.* **1978**, *69*, 2514.

integrations of the Oregonator. We assume that the relaxation amplitudes of the model are too small to be observed in comparison to the amplitude of the damped oscillator. Furthermore, the Oregonator model does not include the complex organic chemistry involved in malonic acid oxidation. The relationship of the damping constant with other kinetic variables such as concentrations and k_f values is extremely complex for the Oregonator model and may not be given by a simple closed-form expression.

Entrainment of the BZ reaction was measured experimentally[6] and calculated under conditions for which the Oregonator shows limit cycle oscillations (in the *absence* of external Br^-). Since the free-running BZ oscillations are nonsinusoidal and complex, there appears to be some ambiguity in the quantitative interpretation of entrainment in this case.

Further work on the influence of forcing amplitude, flow rate, concentrations, and temperature is in progress.

Acknowledgment. We thank the Fonds der Chemischen Industrie for partial support of this work.

(6) Thönnissen, H., Zulassungsarbeit, University of Würzburg, 1983.

Reaction of Fluorine Atoms with Alkyl Iodides: A Possible Observation of the Walden Inversion in the Gas Phase

T. V. Venkitachalam, P. Das, and R. Bersohn*

Department of Chemistry, Columbia University
New York, New York 10027

Received May 23, 1983

When fluorine atoms attack methyl iodide molecules, three reactions are possible:

$$F + CH_3I \xrightarrow{1} CH_3 + IF \qquad \Delta D_0^\circ = -10.3\text{kcal/mol}^1 \qquad (1)$$

$$F + CH_3I \xrightarrow{2} CH_2I + HF \qquad \Delta D_0^\circ = -36.5\ \text{kcal/mol} \qquad (2)$$

$$F + CH_3I \xrightarrow{3} CH_3F + I \qquad \Delta D_0^\circ = -70.9\text{kcal/mol} \qquad (3)$$

Reaction 1 has been studied by crossed molecular beams[2] and by laser-induced fluorescence of the IF product.[3] In this communication we show that reaction 3 does occur and present some evidence that the Walden inversion takes place in the gas phase. This system of reactions has been studied by mass spectrometric analysis of a flowing reaction system.[4] The overall rate constant $k = k_1 + k_2 + k_3$ is 2×10^{-10} cm^3/(molecule s), and k_3 was estimated to be $<0.3k$. Studies with ^{18}F atoms have shown that the rate constant for reaction 3 is $8 \pm 3 \times 10^{-13}$ cm^3/molecules·s.[9]

A two-photon laser-induced fluorescence technique[5] has been recently developed for detecting iodine atoms in either the $^2P_{3/2}(I)$ or the $^2P_{1/2}(I^*)$ state. In this method two photons are absorbed at 304.7 and 306.7 nm by the I and I* atoms, respectively. The excited iodine atoms emit an infrared photon followed by a vacuum ultraviolet photon, which is detected.

In our experiments SF_6 and an alkyl iodide at equal pressures were mixed and flowed through a reaction vessel at a total pressure of 0.2 torr. A CO_2 laser pulse (0.5-μs duration, 10.6 μm, 0.5 J/pulse) dissociated the SF_6 to F and SF_5. One microsecond later a dye laser was fired. At these low pressures and short times single collisions predominate. The experiment was repeated at 5 Hz while the dye laser was gradually swept through the I and I* absorption peaks at 304.7 and 306.7 nm. The resulting fluorescence intensities for the I and I* atoms are shown in Figure 1 for methyl, ethyl, isopropyl, and *tert*-butyl iodide. From the relative intensities one sees that a tertiary iodide does not give iodine atoms, a secondary iodide does give some, and a primary iodide gives much more. An exactly parallel behavior is shown by the Walden inversion in solution. The ratio I*/I is 0.42 ± 0.14 for CH_3I, 0.32 ± 0.13 for C_2H_5I, and 0 for i-C_3H_7I.

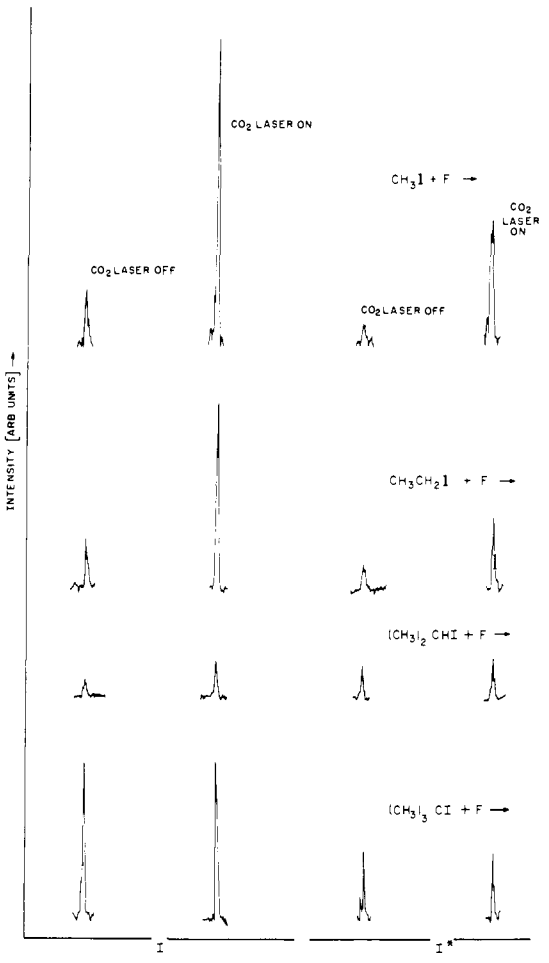

Figure 1.

Tests were made to show that the iodine atoms were not photodissociated from the alkyl iodide by the CO_2 laser or by two-photon dissociation by the dye laser of the radical product of reaction 2 or of the IF product of reaction 1. In the absence of SF_6, CO_2 laser pulses did not produce additional iodine atoms. Moreover when the delay time between the CO_2 and dye-laser pulses was lengthened from 0.5 to 1.0 μs the iodine atom signal increased showing that iodine atoms are generated by collisions. Besides the iodine atoms produced by reactive collisions, iodine atoms are also produced during the probing pulse by a two-photon absorption by the alkyl iodide. The contribution that these latter iodine atoms make to the observed iodine fluorescence signal is a result of two successive two-photon absorptions. The dye-laser power is adjusted so that the iodine atom fluorescence with the CO_2 laser on is maximized relative to that with the CO_2 laser off. The radical products such as CH_2I are much less abundant than the parent and presumably have similar absorption coefficients at the probing wavelengths. As for IF, strong laser-induced fluorescence signals were seen for it from the alkyl iodides discussed here and also CF_3I but iodine atom signals were not seen for t-BuI and CF_3I. Experiments at 100 mtorr of CH_3I and SF_6 pressures varying between 25 and 125 mtorr showed that the I atom fluorescence intensities varied linearly with the SF_6 pressure

(1) Thermochemical data are from: Okake, H. "Photochemistry of Small Molecules"; Wiley: New York, 1978.
(2) Farrar, J. M.; Lee, Y. T. *J. Chem. Phys.* **1975**, *63*, 3639.
(3) Stein, L., Wanner, J.; Walther, H. *J. Chem. Phys.* **1980**, *72*, 1128.
(4) Leipunskii, I. O.; Morozov, I. I.; Tal'Roze, V. L. Dokl. Chem. (*Engl. Transl.*) **1971**, *198*, 1367.
(5) Brewer, P.; Das, P.; Ondrey, G.; Bersohn, R. *J. Chem. Phys.* **1983**, *79*, 720.
(6) Brooks, P. R.; Jones, E. M. *J. Chem. Phys.* **1966**, *45*, 3449.
(7) Parker, D. H.; Chakravorty, K. K.; Bernstein, R. B. *Chem. Phys. Lett.* **1982**, *86*, 113.

0002-7863/83/1505-7452$01.50/0